AUT Journal of Mechanical Engineering

AUT J. Mech. Eng., 5(1) (2021) 173-190
DOI: 10.22060/ajme.2020.17224.5850

Assessment of Fountain Flow Effects on Two Non-Overlap Tandem Rotors Performance

A. Mehrabi, A. R. Davari*

Department of Aerospace Engineering, Science and Research Branch, Islamic Azad University, Tehran, Iran

ABSTRACT: Very few issues are yet to be reported about the fountain flow beneath the tandem rotors configuration body in ground effect. In this paper, a series of tests have been performed using multipurpose test stand to study the fountain flow pattern of a sub-scale model of a generic tandem rotor helicopter in ground effect. Pressure and velocity measurements were performed by the pressure ports embedded longitudinally along a generic tandem rotor helicopter fuselage. The presence of a second rotor in tandem rotors configuration causes a fountain flow formation in the longitudinal center region below the helicopter and a semi-quiescent flow was there. The positive effects of this flow were detected such as increasing the sub-body pressure lifting force, the pressure distribution balance, and reinforcing the lift by the formation of the positive pressure gradient on sidewalls of the airframe. Tuft test observations confirmed the location of the fountain flow formation concluded from pressure and velocity measurements. The mentioned fountain flow aerodynamic effects must be taken into account in the tandem rotor helicopter flight controls trims, stability, and control augmentation system and lift force calculations.

Review History:
Received:15/10/2019
Revised: 07/02/2020
Accepted:10/03/2020
Available Online: 19/03/2020

Keywords:
Pressure Distribution
Lift force
Non-overlapping Tandem Rotor;
Fountain Flow
Helicopter

1. INTRODUCTION

1.1. In Ground Effect Hover

A deeper understanding of the unsteady aerodynamics of tandem rotor helicopters, which was started in past decades, shed new light on the issue of their performance. For a helicopter flying near the ground, the direction of flow induced by the rotor changes from vertical downwash to radial outwash due to interactions with the ground. The value of rotor disk loading determines the strength of this induced flow [1]. The outwash starts from the outboard region of the blade tip and flows away from the helicopter, as shown in Fig. 1.

Despite the ground effect is a well-known issue in helicopter performance, it is necessary that some remained dark corners of the aerodynamics behavior of tandem rotors in ground effect should be discovered. The ground effect is one of the primary concerns during actual flight and also in a wind tunnel or hovering tests. For heights less than one rotor diameter above the ground, the hovering performance is strongly affected by the ground effect [3].

1.2. Fountain Flow

The flow-field around the tandem rotor systems can be divided into five regions, based on the dominant phenomena in each region. There can be seen a relatively quiescent flow region under the helicopter that is likely to be similar to a fountain flow, even though no measurements have already been reported to confirm this hypothesis. In the literature, this region is known as the Fountain flow and is formed below the intersection of the two rotors where the flow is upward [4].

While a tandem rotor configuration hovers and two rotors are positioned so that there is no overlap between them, there is a clear distance between them, in the upper surface of the airframe the downwash and spanwise flows from the blade tip vortices merge at the centerline of the fuselage and will form an upward unsteady fountain flow (Fig.2). This flow gets recirculated into the rotors and has a significant influence on the aerodynamic performance of the rotors. In hover, the upper Fountain flow causes a vertical drag force on the fuselage, which is called download [5]. The experiments made to measure the download on the wings of tilt rotors in helicopter mode showed that the amount of its reverse effect was equal to 10-15% of the total rotor thrust and reduces the vehicle payload in hover Out of Ground Effect (OGE) [6-8].

When the helicopter hovers In-Ground Effect (IGE), the presence of the ground influences the wake of the rotors under the fuselage (Fig.2). A large part of the wakes of the tandem rotors spanwise flows recirculate as they interact with the ground surface and meet under

*Corresponding author's email: ardavari@srbiau.ac.ir

the longitudinal centerline of the fuselage and form a Fountain flow in a similar form to what happens on the upper surface of the fuselage [9]. This Fountain flow will be trapped under the bottom surface of the fuselage and causes an upward force on the helicopter and reduces the download on the fuselage caused by upper surface fountain flow. Some measurements show that this positive upward force, could be as high as 9% of the rotor total thrust in tilt rotors in their helicopter mode [10]. So, in contrary to thrust reduction due to the Fountain flow in the upper surface of the fuselage, below the helicopter fuselage, the Fountain flow increases the lifting capacity and payload beyond the maximum thrust of the rotors.

Clearly, it is very important to know the effects of this flow on the performance of the tandem rotors in different positions to achieve better performance in the hover mode. It seems that the flow pattern of the Fountain flow in tandem rotors varies with having overlap or without overlap. Investigating the effects of distance between tandem rotors and the ground effect on the pressure and velocity values of the Fountain flow below the generic tandem model is the main topic of the present study.

For a single rotor operating near the ground, the direction of the downwash flow in the vicinity of the ground rapidly changes from vertical to radial along the surface, extending away from the disk area. This region encompasses many turbulent vortices within the boundary layer with a wide range of length scales. When the rotor height above the ground decreases, it has been observed that the vortex sheet will stretch with higher swirl velocities, resulting in less viscous diffusion and an increasing number of the pairing tip vortices [11]. This process preserves a much longer vortex core original shape against the changes and preserves its original shape [12]. It is expected that the effects of this physical behavior of the flow will also be observed under the helicopter airframe which leads to the formation of a Fountain flow. The tip vortices and the vortex sheets along with pressure jump across the blades, impart remarkable oscillations in the velocity which must be taken into account in rotor Fountain flow measurements.

1.3. Research Background

The results of studies show that the ground effect on tandem rotor configurations cannot be modeled by linear functions of such independent variables as thrust or height of rotors from the ground. Moreover, there are still several unknown issues about the tandem rotor configurations which need to be discovered. For instance, in a tandem rotor system, there is a strong interaction between the induced flows of the rotors. Several experimental and numerical surveys are still needed to develop the existing understanding of the tandem rotor configurations performance.

Several surveys have been devoted to analyzing the performance of tandem rotors [13, 14]. Ramasamy [9] studied the downwash and outwash flow behavior by conducted experiments using a sub-scale CH-47D helicopter measuring the flow-field velocities in a vertical plane at several azimuth angles and various radial distances from the rotor axis, using the particle image velocimetry technique. He reported that there is a relatively quiescent flow region under the airframe that is likely to be similar to a Fountain flow, but he didn't perform any measurement on that region.

Some studies on the upper Fountain flow of tilt-rotors in helicopter mode and side-by-side rotors were conducted to identify and reduce resultant downloads and their unfavorable consequences. These experiments were on major subjects like as effect of the tilt-rotor wing geometry on download value, the effect of the rotor location on fountain flow, download force, and the effect of parameters such as ground effect on Fountain flow of actual tilt rotor configurations. It is important to note that in ground effect, contrary to the mentioned configurations, the Fountain flow-field of the tandem rotors, even their non-overlap type is more complex. Because in the side-by-side arrangement of the tilt rotors, each rotor is less affected by the wake of the other one, but in the tandem arrangement, each rotor is affected by vortices of other rotor's wake.

Fountain flow velocities of a full-span and a semi-span configuration with an image plane of a sub-scale model of the XV-15 tilt rotor measured by hot-wire technique in reference [8]. It was observed that flow velocities have significant differences in the upper Fountain-flow region in comparison with other azimuth angles. It should be noted that the Fountain flow is a free jet, so the flow behavior changes by the shear layer that forms on an image plane that was used and it is not actual.

In recent years, with the advent of digital computers and numerical algorithms, valuable information has been obtained using computational fluid dynamics [15, 16]. However, accurate enough predictions at a reasonable computational time and costs are still challenging issues [17]. Care must be taken in mesh generation and choice of turbulence model to properly capture the details of such complicated phenomena as Fountain flow and the rotor wake structure [18]. The comparison of the results of the numerical studies with experimental data and actual results has shown the significant progress of these methods and their success in simulating and predicting aerodynamic details of Fountain flow [19, 20], but in comparison to the experimental results there are still some offsets in the numerical simulation due to the blade tip vortices, downwash interference with the airframe and the aerodynamic properties of the blades [16, 21].

Reviewed studies showed that Fountain flow between the tandem rotor configurations is a missing phenomenon in previous reports and no case has been

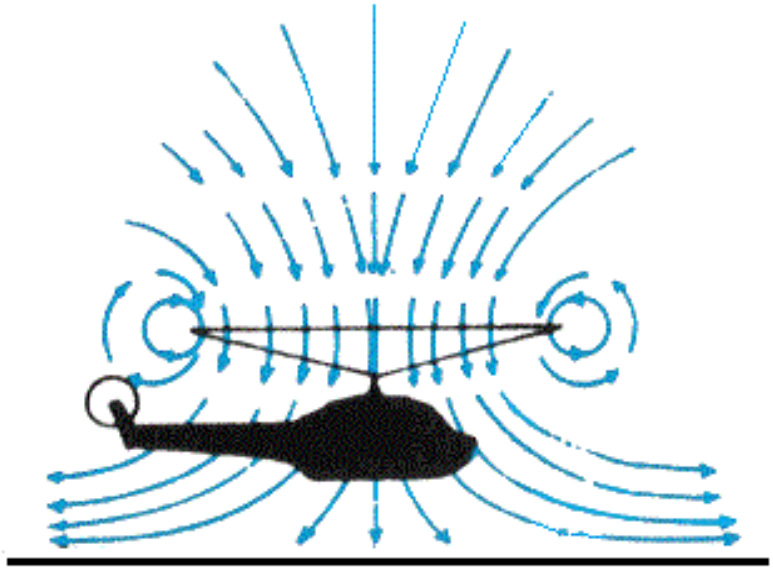

Fig. 1. In-ground effect hover [2]

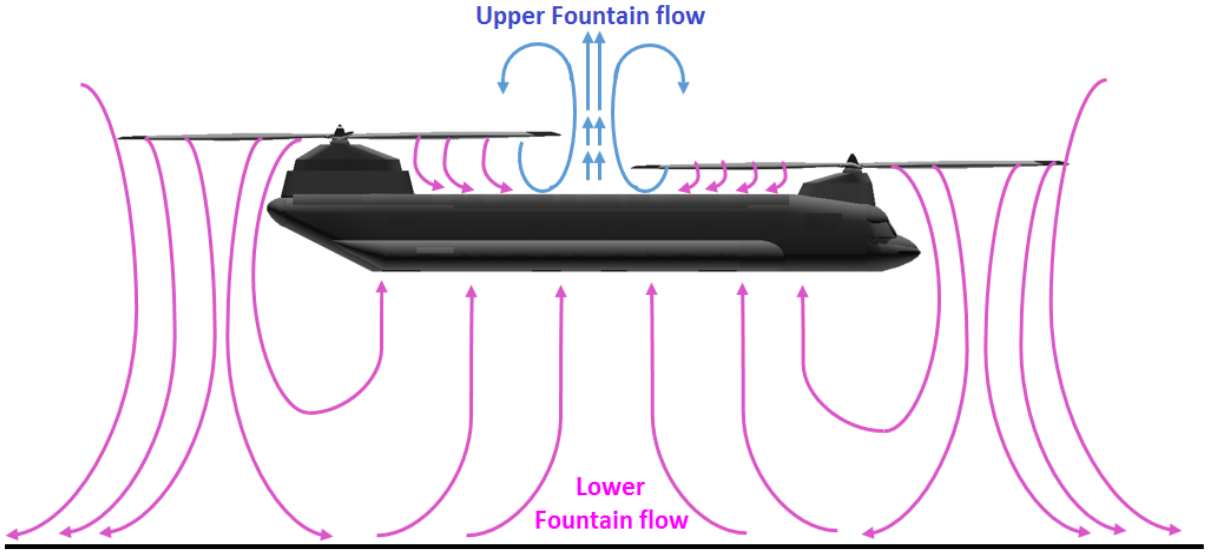

Fig. 2. Non- overlap tandem rotor fountain flow IGE.

reported on experimental investigations relating to that. On the other hand, most of the experimental investigations already reported, have been performed in wind tunnels or special hover chambers in which, the flow recirculated by the chamber or tunnel walls, deteriorates the flow-field and makes it different from that occurs in a real flight [13, 14, 22]. In the simulation of free flow on the rotors, the effects of the tunnel walls can hardly be eliminated. Despite using various methods to remove the effects of the boundary layer on wind tunnel or chamber walls, a majority of the discrepancies observed between the wall-confined experimental data and those obtained during actual tests are believed to be due to the wall effects [23, 24]. Very limited works were devoted to a detailed study of the effects of tandem rotor elevation from the ground on the flow-field. This necessitates a large test section wind tunnel to eliminate any wall interaction and blockage effects.

To avoid the remarkable costs of such tunnel and the consequent problems such as its turbulence level, velocity limitations, etc, a versatile test stand has been used in the present study to investigate the fountain flow

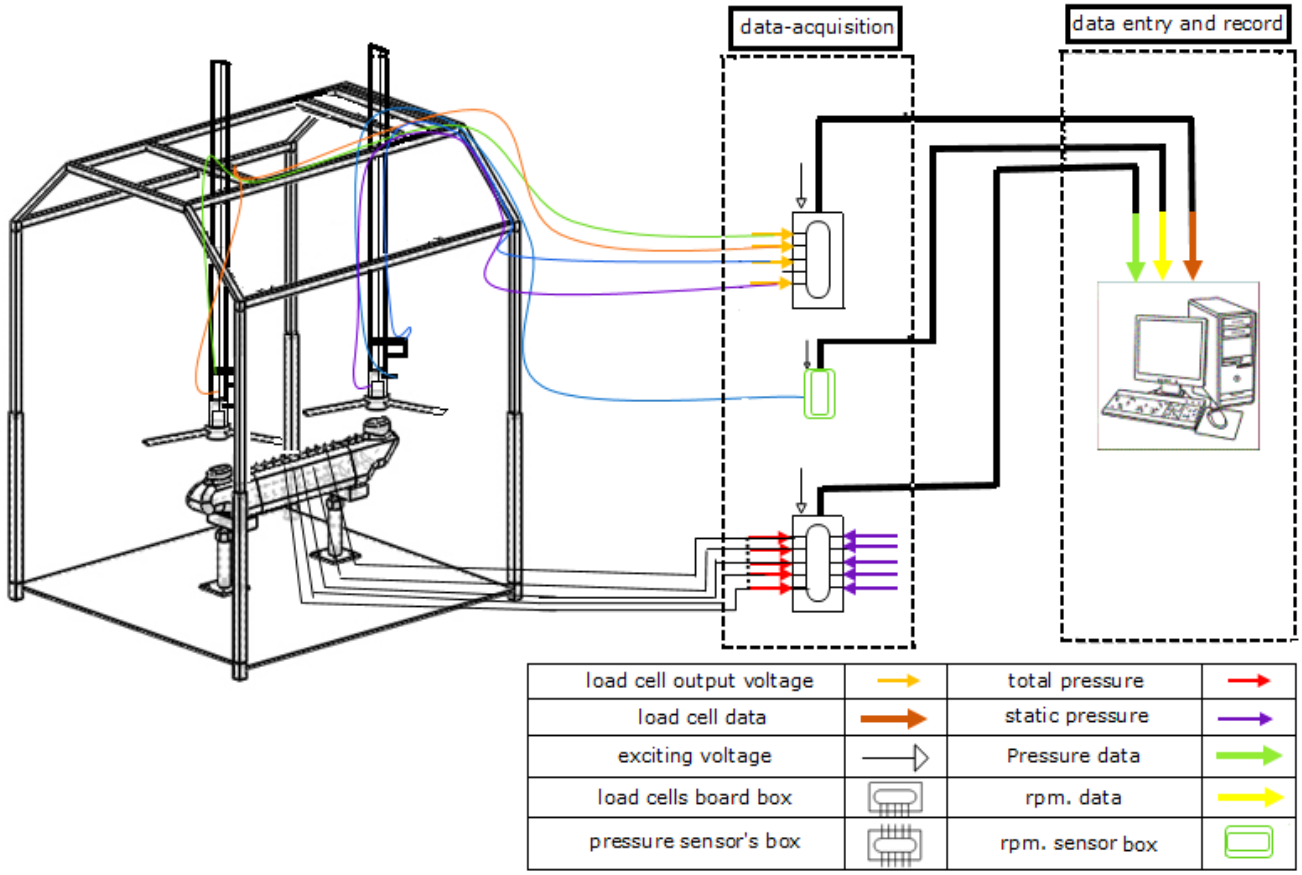

Fig. 3. The overall schematic view of the present test rig.

characteristics below a subscale twin-rotor airframe in the absence of any ambient wind, with no surrounding wall effects. Various hovering elevations can be examined both in-ground effect and outside it. This test rig is capable of measuring the pressure and velocity distributions in hover. So, in this paper, the effects of a complete body and tandem rotor configuration have been studied on the Fountain flow behavior of a detailed sub-scale model at two different heights above the ground. The flow visualization under the model airframe was conducted by the tuft technique to investigate the flow pattern changes caused by impacting flow. Tuft flow visualization techniques were used in some prior studies to investigate the characteristics of downwash and outwash of model and full-scale single main rotor helicopters and tilt rotors [6, 23, 25]. The present experiments have been performed in a big test room with a width of 7.3m, a length of 9.1m, and a height of 3.5m in the absence of the ambient winds and according to test conditions, the measured turbulence intensity of the incoming flow was less than 2%.

2. EXPERIMENTAL SETUP

The overall test rig encompasses three subsystems: the main stand, the data-acquisition section, and data entry and record section, shown in Fig.3. Motor modules, the fuselage, rotors, and pressure sensor tubes are installed in the main stand. The main stand height can be changed vertically to simulate the ground effect.

To generate the power needed to rotate the rotors, two EMAX brushless motors BL4030 were used, with a maximum rotational speed of approximately 4000 rpm. These motors are mounted on a test rig using a lightweight aluminum mount and two rails. The most important advantage of these types of motors is that they have a much higher power-to-weight ratio.

The boxes of the pressure sensors and signal amplifiers are located in the data-acquisition section. Sixteen pieces of precise and sensitive MPXV7002 differential pressure sensors were employed to measure the pressures incoming through ports (Fig.4). This transducer combines advanced micromachining techniques, thin-film metallization, and bipolar

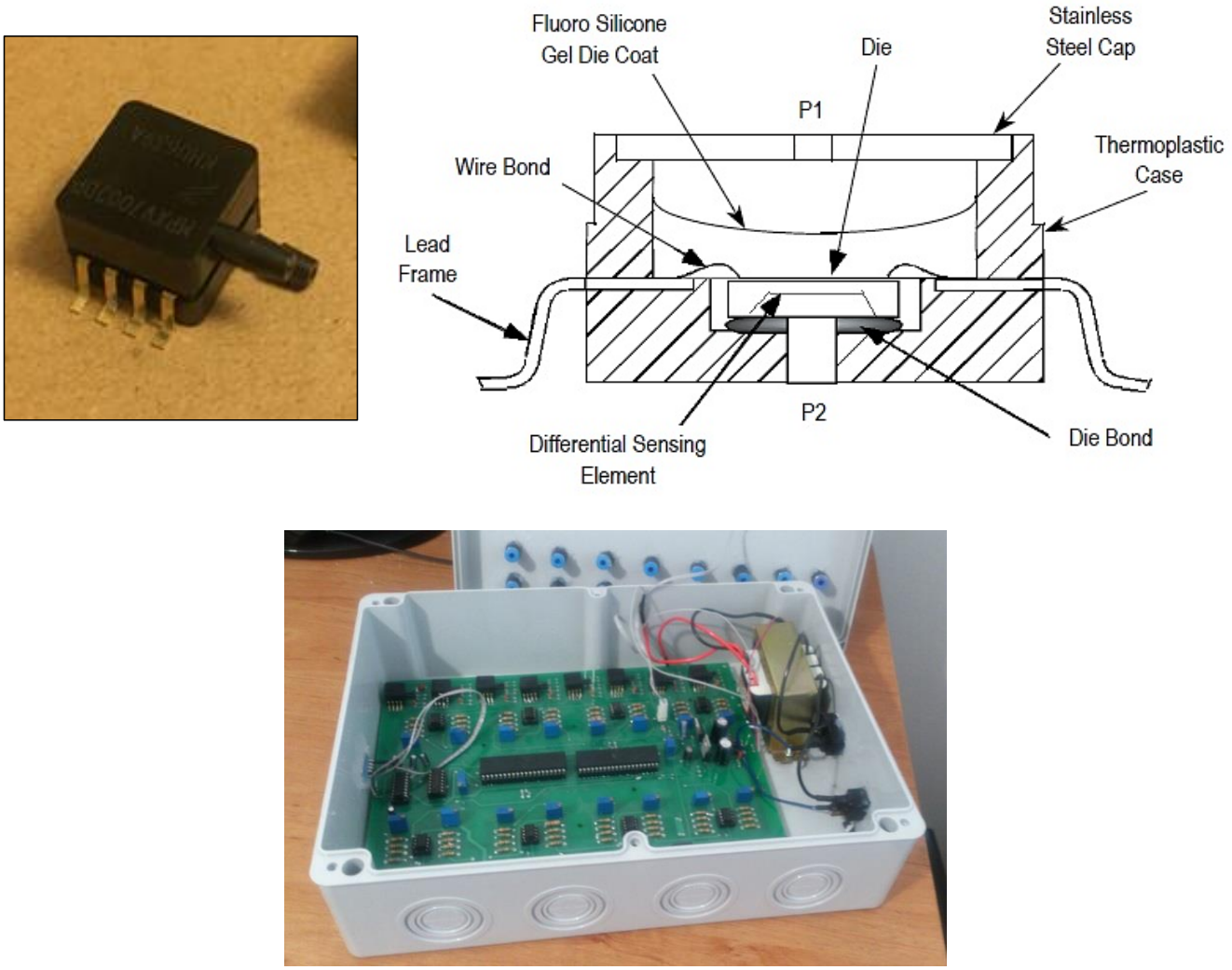

Fig. 4. Differential pressure sensors.

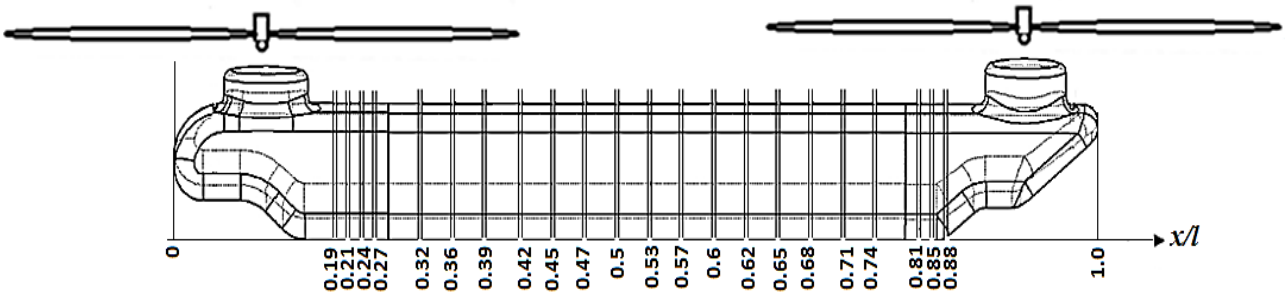

Fig. 5. The schematic view of tandem rotors arrangement and the longitudinal position of the pressure ports.

processing to provide an accurate, high-level analog output signal that is proportional to the applied pressure. The total pressure of the test environment is sensed by one port and the static pressure by the other port of the differential pressure sensor. The difference between these two pressures stimulates the internal diaphragm of the sensor and generates the output voltage.

The data recording rate of the pressure sensors was 22 data records per second. In conducted experiments, the data were acquired for 35 seconds in each test so, 770 samples have been recorded. This sampling rate is enough to capture the periodic variations and unsteadiness in the flow-field. Pressure range of the pressure sensors is -2.0 to +2.0kPa. Their response time and warm-up time are 1.0 and 20ms respectively. Typical error of the pressure sensors over +10°C to +60°C is 2.5%, with auto-zero system, and 6.25% maximum error without auto zero. Auto-zero is defined as storing the zero pressure output reading and subtracting this from the device's output during normal operations.

Pressure ports are embedded along the longitudinal centerline of the fuselage to measure the pressure and velocity distribution below the body of the model. The ports have been located at specified distances from each other. The port arrangement is shown in Fig. 5. The ports consist of tiny steel probes of 2.5mm external

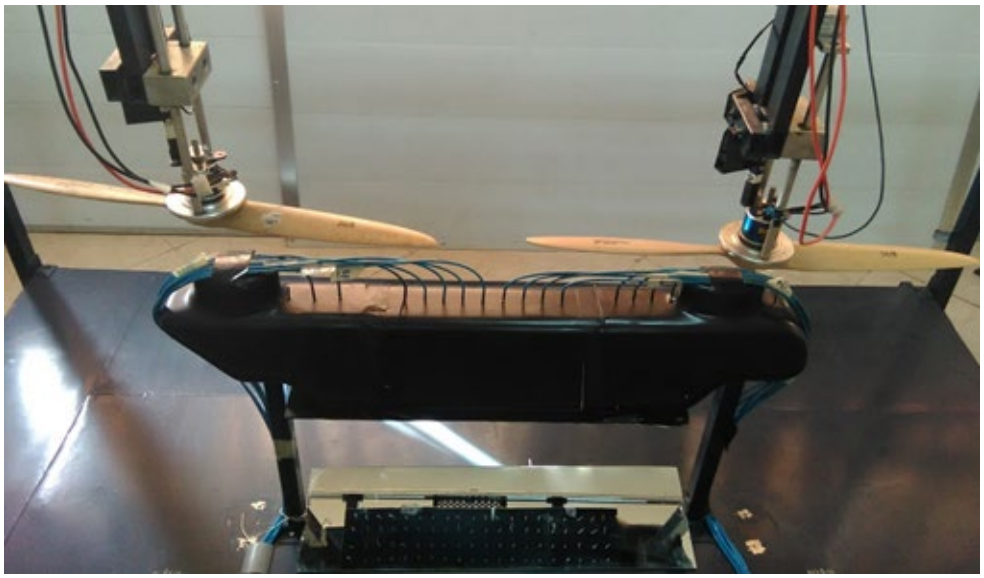

Fig. 6. The white tufts planted at the bottom surface of the model body.

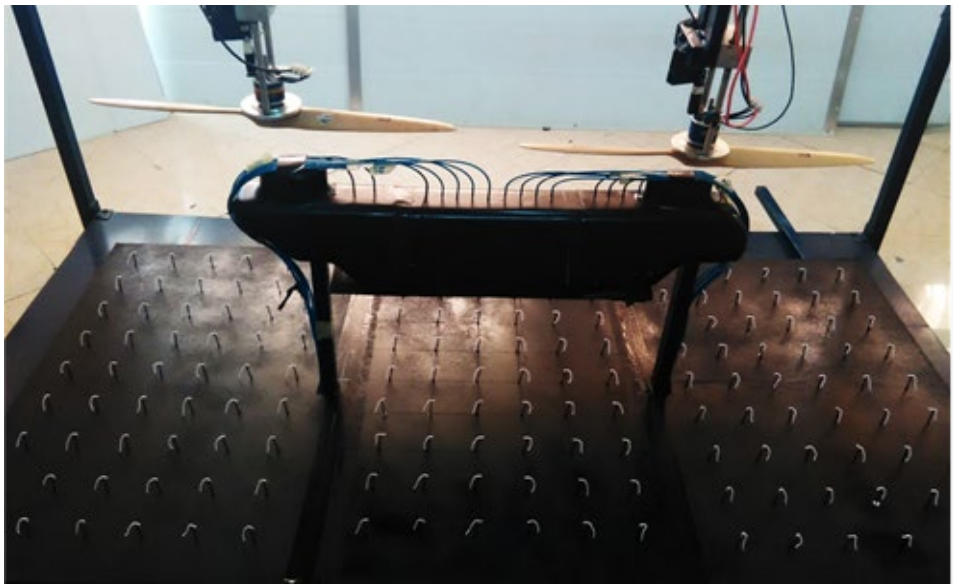

Fig. 7. White tuft flags planted at the black plane on the ground.

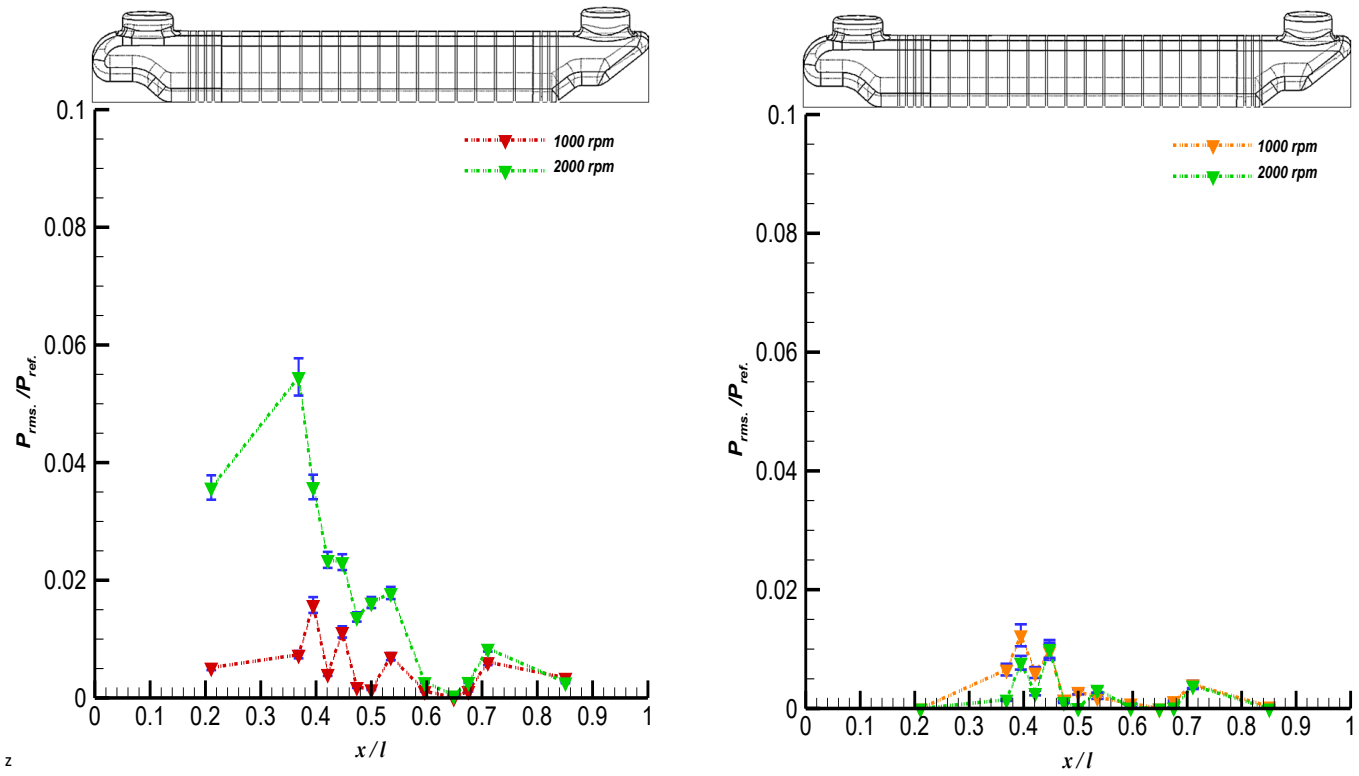

(a). h/2R= 0.5 (b). h/2R=1

Fig. 8. Impact flow RMS pressure distribution below the fuselage in single rotor operation

and 1.5mm internal diameter. The probes were mounted in a way that they are fully tangent to the underside of the airframe, each was almost 3.5cm apart except where the main body parts are connected. Each probe was directly connected to a differential pressure transducer via a plastic tube.

The purpose of the present study is to measure the pressure and velocity changes caused by Fountain flow at different points below the fuselage of a non-overlapping tandem arrangement and investigate the blades' aerodynamic interaction on the Fountain flow pattern by flow visualization. Two sets of constant pitch rotor blades were employed. The rotors were 66.4cm in diameter. A schematic view of the tandem rotors arrangement and the longitudinal position of the associated pressure ports shown in Fig. 5. Two sets of tests were performed; the first set of tests done using a single (forward) rotor and then, and the second set of tests were done by tandem rotors. The experiments were carried out for two vertical distances from the ground; $h/2R$=0.5 and $h/2R$=1. Both single and tandem rotor configurations have been tested to compare the fountain flow-fields as well as the ground proximity effects.

In order to physically understand the airflow patterns leading to the fountain flow, special tuft flow visualization techniques were used in the present study. A series of white tufts planted at the black background were attached to the bottom surface of the body (Fig.6). The tufts were 2.5cm in length and were arranged in 3cm square grids. Another white tuft flag planted at the black plane on the ground to complete flow capturing below the rotors (Fig.7). The tufts in this plane were 4.5cm in length and were mounted on very thin wooden rods at a height of 5cm like a flag. They were arranged in 10cm square grids. The tufts were extremely light and flexible so that they would move freely with the flow field.

For rotors operating near the ground, because the turbulent vortices motions associated with eddies within the boundary layer are approximately random, we can characterize them using statistical concepts. Flow pressure and velocity records include both mean and turbulent components. The flow decomposed in Eq. (1) is as follows:

$$P(t) = \bar{p} + p'(t)$$
$$v(t) = \bar{v} + v'(t) \quad (1)$$

In theory, the pressure and velocity record are continuous and the mean can be evaluated through

integration. However, in experiments, the measured pressure and velocity records are a series of discrete points, p_i and u_i. In equations, an over bar is used to denote a time average over the time interval t to $t+T$, where T is much longer than any turbulence time scale but much shorter than the time-scale for mean flow unsteadiness.

The mean velocity was calculated as Eq. (2).

$$\bar{p}(t)=\frac{1}{N}\sum_{1}^{N}p_i(t)$$
$$\bar{v}(t)=\frac{1}{N}\sum_{1}^{N}v_i(t) \quad (2)$$

where $p_i(t)$and $v_i(t)$ are the pressure and velocity at time t of record i and N is the number of records to be included in the calculation.

The turbulent fluctuations were calculated by subtracting the mean value from each individual instantaneous value as given in Eq. (3).

$$p_i'=p_i(t)-\bar{p}(t)$$
$$v_i'=v_i(t)-\bar{v}(t) \quad (3)$$

The root-mean-square values are used as the standard deviation of the set of "random" pressure velocity fluctuations (p_i' and v_i'). So, the P_{rms} and V_{rms} were calculated as Eq. (4) [26]:

$$P_{rms}=\sqrt{\frac{1}{N}\sum_{1}^{N}(p_i')^2}$$
$$V_{rms}=\sqrt{\frac{1}{N}\sum_{1}^{N}(v_i')^2} \quad (4)$$

3. RESULTS AND DISCUSSION

The tests and results in this study have three main subjects: the Fountain flow pressure and velocity variations in different longitudinal points under the helicopter body, the influence of the rotors aerodynamic interaction on Fountain flow, and the flow visualization by using the tuft method.

3.1.Fountain Flow Pressure And Velocity Variations Under The Airframe

Fig. 8 shows the flow pressure distribution under the helicopter body, while only the forward rotor was rotating which simulates the baseline single-rotor configuration and protects the rotor performance from the induced flow of the other one. The measurements were performed for the forward single rotor rotational speed of 1000rpm and 2000rpm. Note that, ports have been located longitudinally on the centerline of the fuselage. The time-dependent pressure measurements have been performed for several revolution cycles and the P_{rms} and V_{rms} values have been presented in this paper.

For the single rotor for the elevation $h/2R$= 0.5, as the rotational speed of the rotor was equal to 1000rpm, the maximum pressure was recorded approximately in the middle of the body (Fig. 8(a)). As the rotational speed of the single rotor was increased to 2000rpm, the pressure in the points below the rotor increased rapidly. But unlike the previous one, in this situation maximum pressure values occurred near the points below the mid-span of the blade. In areas far from the middle of the body, the increase in rotational speed of the rotor had little effect on the pressure distribution below the airframe, because by moving away from the area below the rotor, due to viscous effects, the blade tip vortices depreciate and then dissipate and become wall jet flow, thus the impact flow to the body would reduce. According to the conceptual pattern of the Fountain flow in-ground effect shown in Fig. 2, the flow caused by the forward blade downwash impacted the front half of the body and has led to an increase in pressure values in these areas.

In Fig. 8(b), when the elevation of the rotor increased to $h/2R$=1, the pressure distribution caused by impact flow decreased and rotational speed of the rotor changes had almost no significant influence on pressure distribution. This can be explained by the decrease in the effect of ground proximity, because when the body and rotor elevation increased, the recirculated flow caused by the ground surface reduced, so the impact flow would reduce. It was also observed that the maximum values of the pressure were recorded in regions below the blade tip and near the middle of the body. This was due to the interaction of the blade wake vortices with the ground and the formation of impact flow in this area. In both cases, the impact flow pressures have been slightly reduced as moving away enough from the rotor.

3.2. Influence Of Rotors´ Aerodynamic Interaction On Fountain Flow

In experiments, the pressure and velocity records showed the turbulent and unsteady behavior of impacting flow below the rotors (Fig. 9), however, the records include both a mean and a turbulent component. In Fig.9, instantaneous values of pressure are shown below the nose, middle, and tail portions of the body. It can be seen that in all diagrams the instantaneous values of pressure and consequently its mean values increase with decreasing rotor height.

The *RMS* values of the Fountain flow pressure for the tandem rotor configuration are shown in Fig. 10. Some differences can be observed in the Fountain flow behavior for tandem configuration comparing to the single rotor baseline, as a result of the flow-field due to the rear rotor and the combinational effects of the twin rotors on the induced flow-field. It was observed that by the addition of the second rotor operation, the pressure distribution due to the Fountain flow was greatly increased, especially this increase was more significant at low elevation when $h/2R$=0.5 (Figs. 10(a,c)).

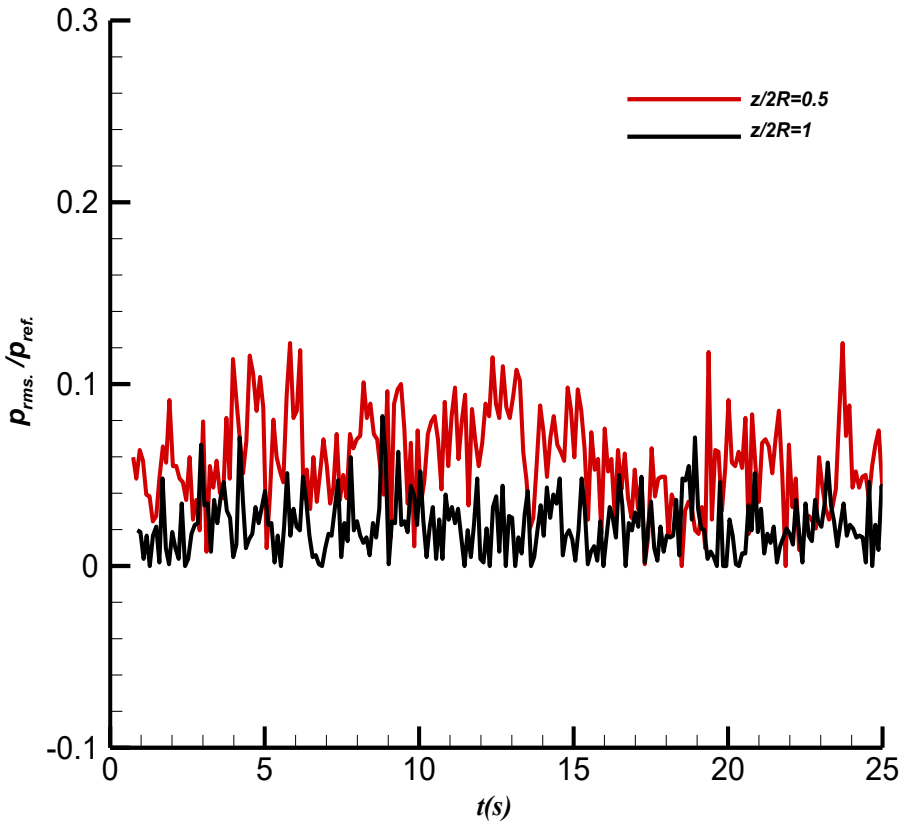

(a). x/l=0.2 , Non-overlapping

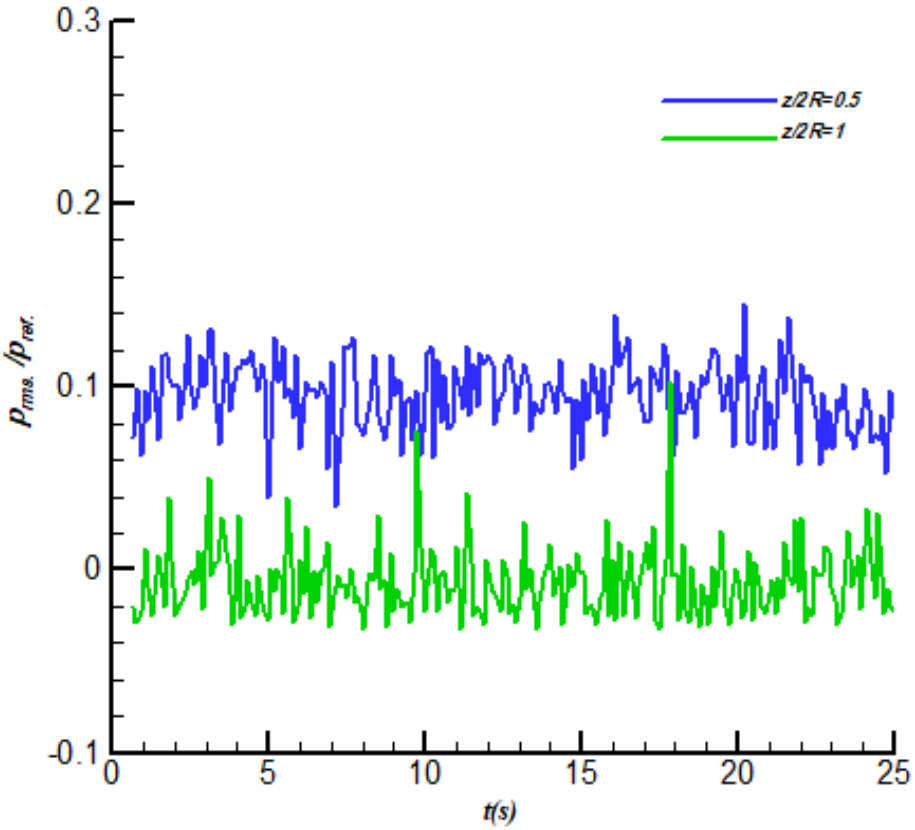

(b). x/l=0.2 , Overlapped

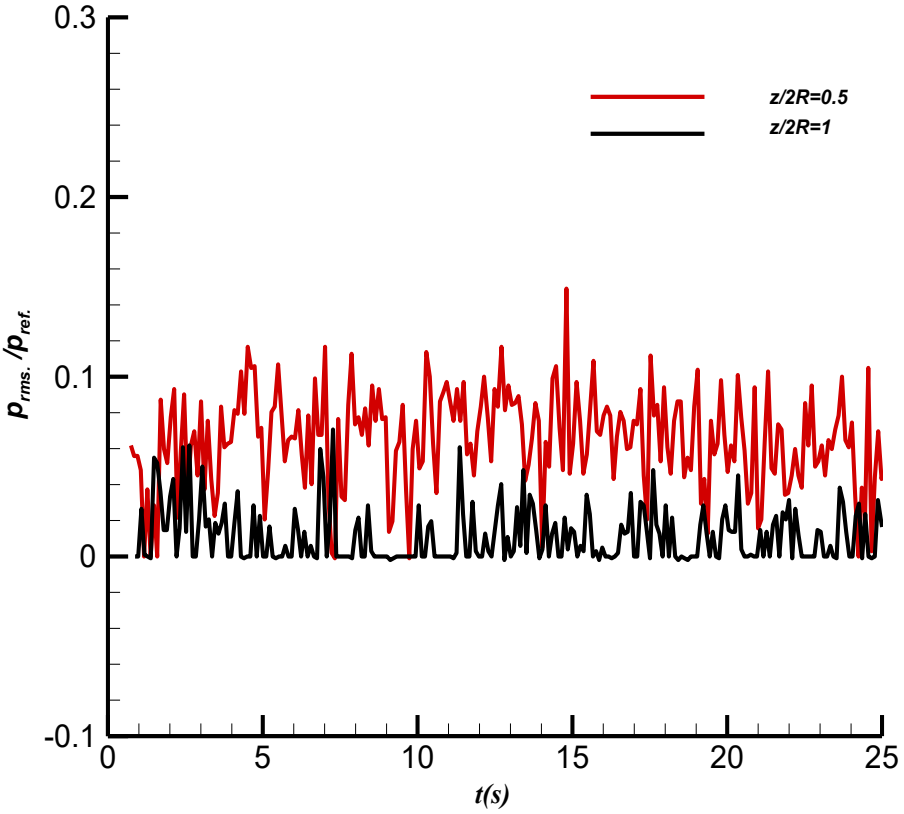

(c). x/l=0.5 , Non-overlapping

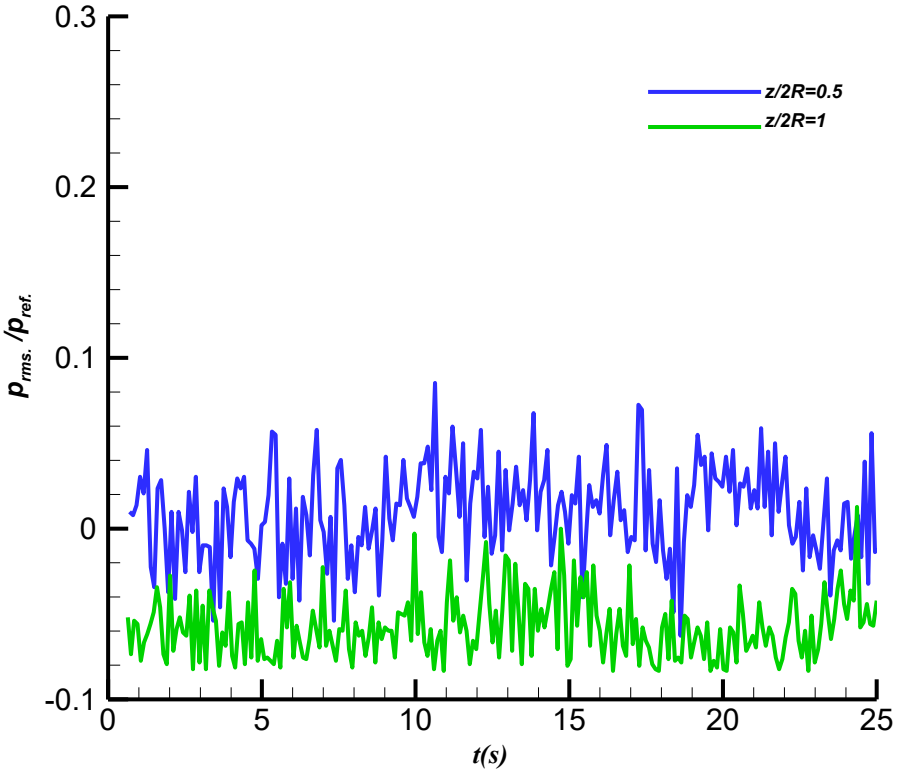

(d). x/l=0.5 , Overlapped

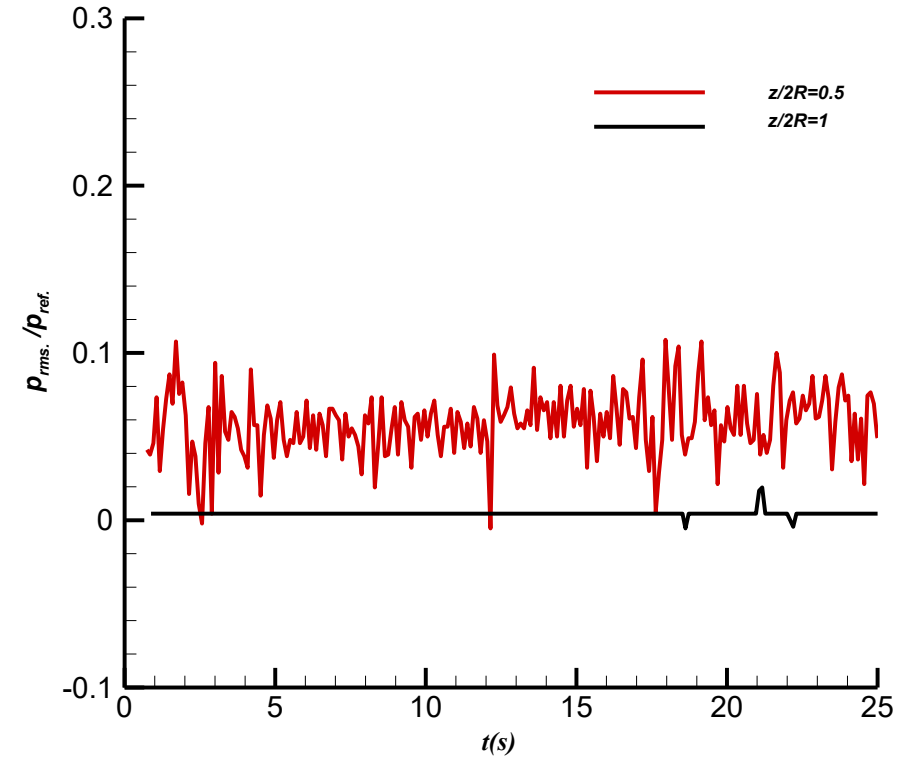

(e). x/l=0.8 , Non-overlapping

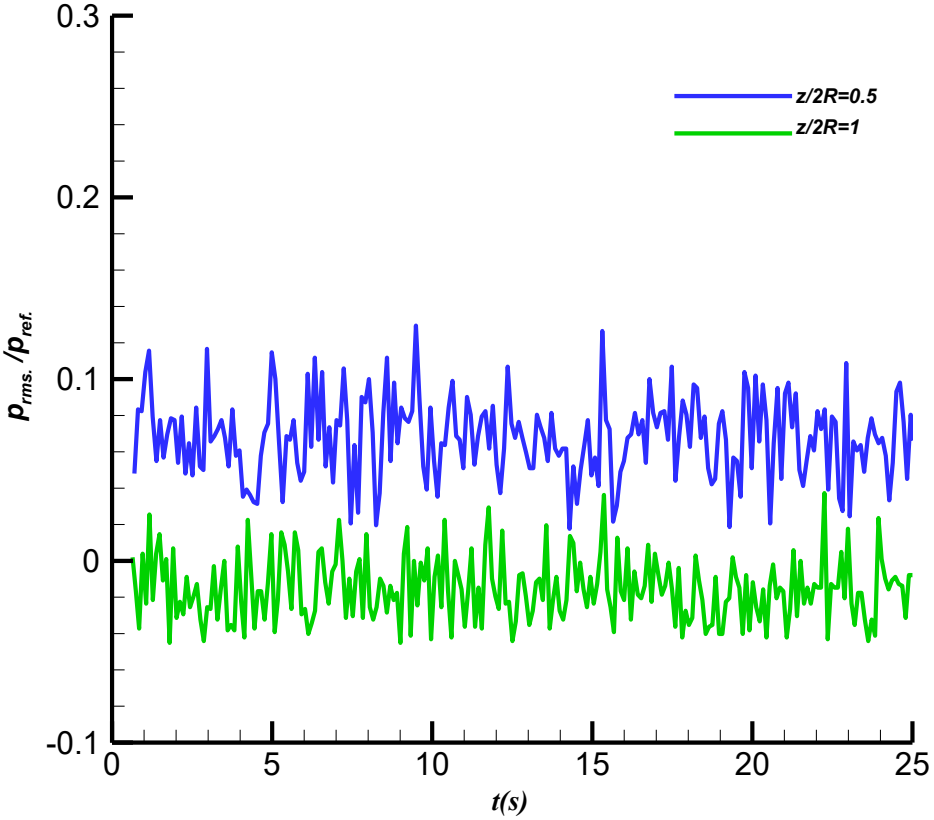

(f). x/l=0.8 , Overlapped

Fig. 9. Time trend of pressure fluctuation between the tandem rotors.

The highlights in Fig. 10 are that, first, as expected, increasing the rotational speed of the rotors had a significant effect on the amount of pressure distribution of the fountain flow. Second, the pressure values slightly increased by decreasing the elevation of rotors and airframe. As seen in the conceptual model presented in Fig. 2, when the elevation of the model decreases, a large part of the wakes of the tandem rotors spanwise flows recirculate, as they interact with the ground surface and meet longitudinal centerline under the fuselage, causes upward pressure on the model. As the elevation of the model increased, the amount of recirculated flow from the ground impact on the bottom of the airframe decreased. On the other hand, due to the decrease in the ground effect, the amount of pairing tip vortices also decreases as well as the coherence of both recirculated flows from the ground also changes so, the location of maximum pressure slightly varied with respect to the previous elevation.

The results in Figs. 10 and 11 show that the overlap between the rotors causes an increase in pressure and velocity values relative to the non-overlapping rotors in both elevations. In all

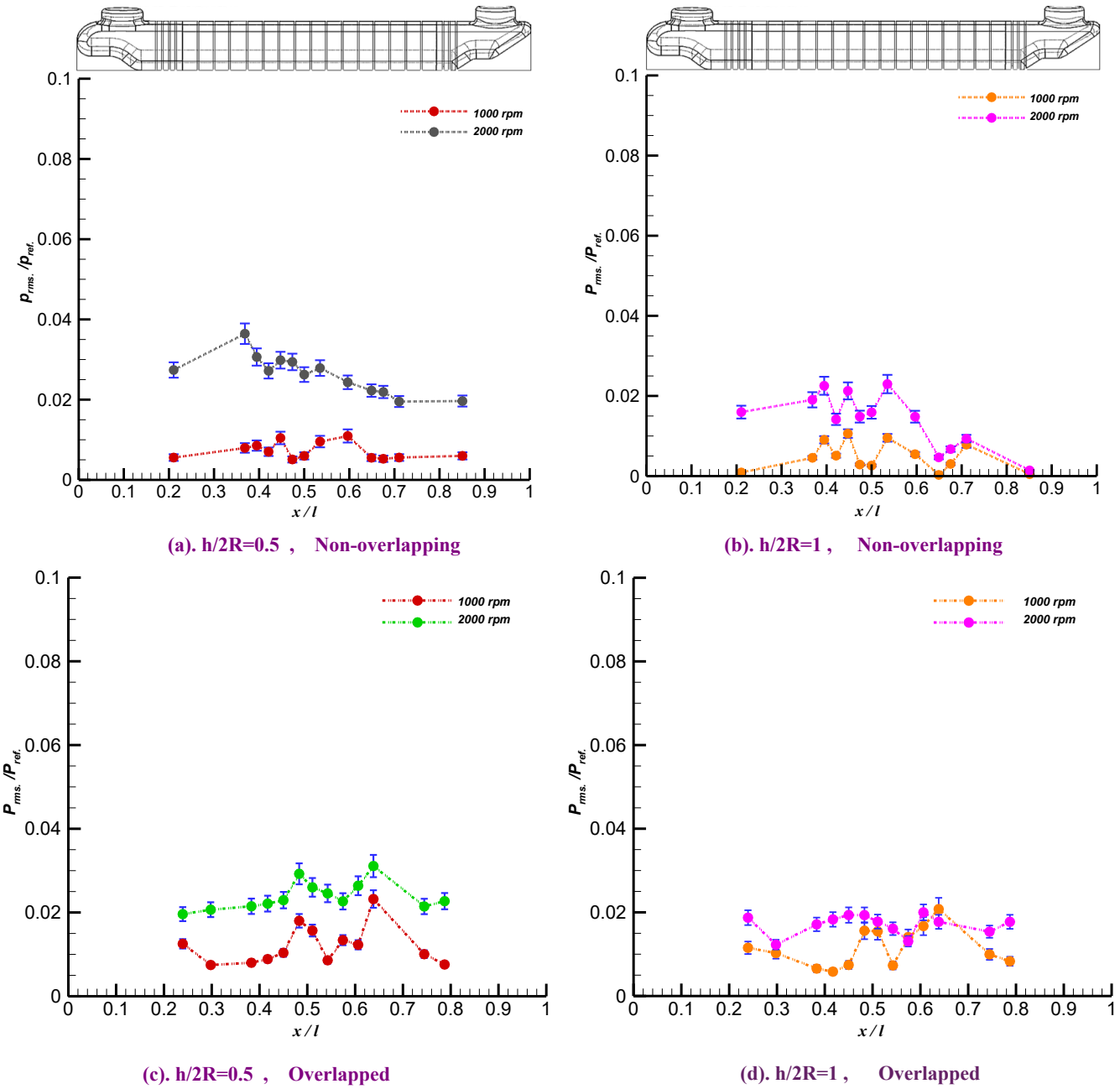

(a). h/2R=0.5 , Non-overlapping

(b). h/2R=1 , Non-overlapping

(c). h/2R=0.5 , Overlapped

(d). h/2R=1 , Overlapped

Fig. 10. Impact flow RMS pressure distribution between the tandem rotors.

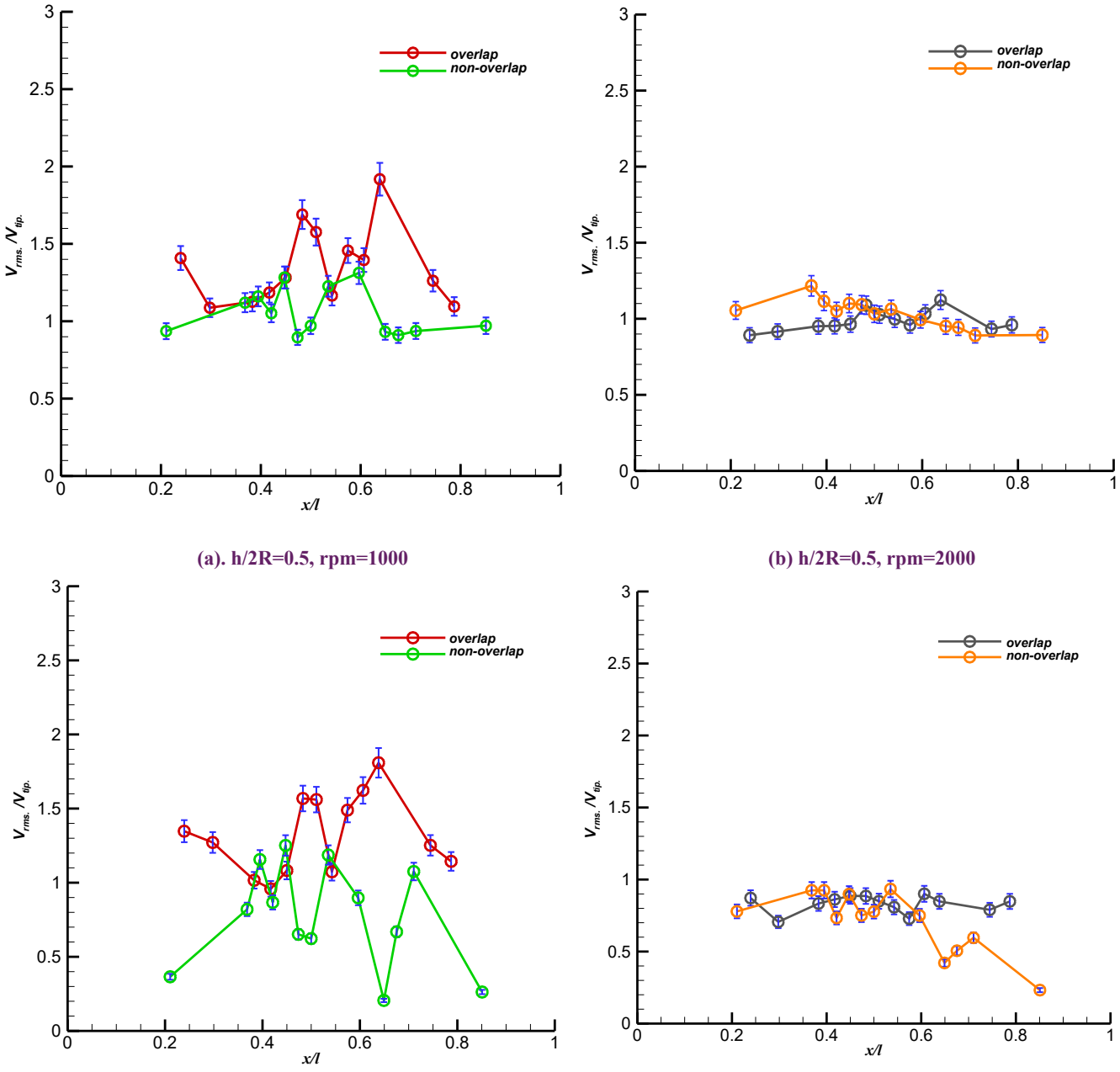

(a). h/2R=0.5, rpm=1000

(b) h/2R=0.5, rpm=2000

(c). h/2R=1, rpm=1000

(d) z/2R=1, rpm=2000

Fig. 11. Impact flow RMS velocity distribution between the tandem rotors

cases, at the central regions, between the rotors, the pressure and velocity values were greater than the other regions.

It can be seen that in each of the diagrams in Fig. 11 there is an area where the velocity values are very low and it can be said that the semi-quiescent flows were in these areas. In the same rotor elevations, semi-quiescent flow spatial extents were located in a specified range in both rotational speeds.

When the model height was h/2R=1 at rpm=1000, in the non-overlap case the spatial extent of the semi-quiescent flow increased slightly but in the overlap case, change in rotors elevations had no significant effect on the semi-quiescent flow range. The cause of this event can be explained by the fact that in the non-overlap case when the model height was increased, due to the decrease in the ground effect, the amount of recirculated flow from the ground surface decreased, so the flow rate also decreased in the area between the two rotors. When

at the given elevation, the rotational speed of the rotor was increased to 2000rpm, due to the increase in the number of blade tip vortices in the wake and the rotor induced downwash flow, the reversed flow from the ground surface increased and the spatial extent of the semi-quiescent flow decreased but in overlap rotors, the clearance between the rotors disappears and there would almost be no way for the flow to escape to upward. As a result, the Fountain flow trapped under the fuselage, consequently, the rotors elevation changes have fewer effects on flow velocity.

3.3. Flow Visualization

In order to physically understand the airflow patterns leading to the Fountain flow, tuft flow visualization technique was used in the present study. To take photos and to record the special operation videos, digital cameras and a mirror on the ground were used to view the flow patterns on the bottom surface of the body (Fig. 6). The tuft experiments were conducted for single rotor and non-overlap tandem rotors in two elevations ($h/2R$=0.5 and $h/2R$=1).

3.3.1. Single Rotor

To simulate the baseline single-rotor configuration which is isolated from the induced flow of the other one, tuft flow visualization was conducted in elevation $h/2R$=0.5 for that. It should be noted that a mirror mounted on the ground was used to movement capture of the tufts, so the quality of the photos was taken by that assistance was declined.

It can be seen from the flow pattern demonstration in Fig. 12 that, when the single rotor was operating, the direction of flow induced by the rotor, due to interactions with the ground, changed from vertical downwash to radial outwash and a large part of the flow at bottom of

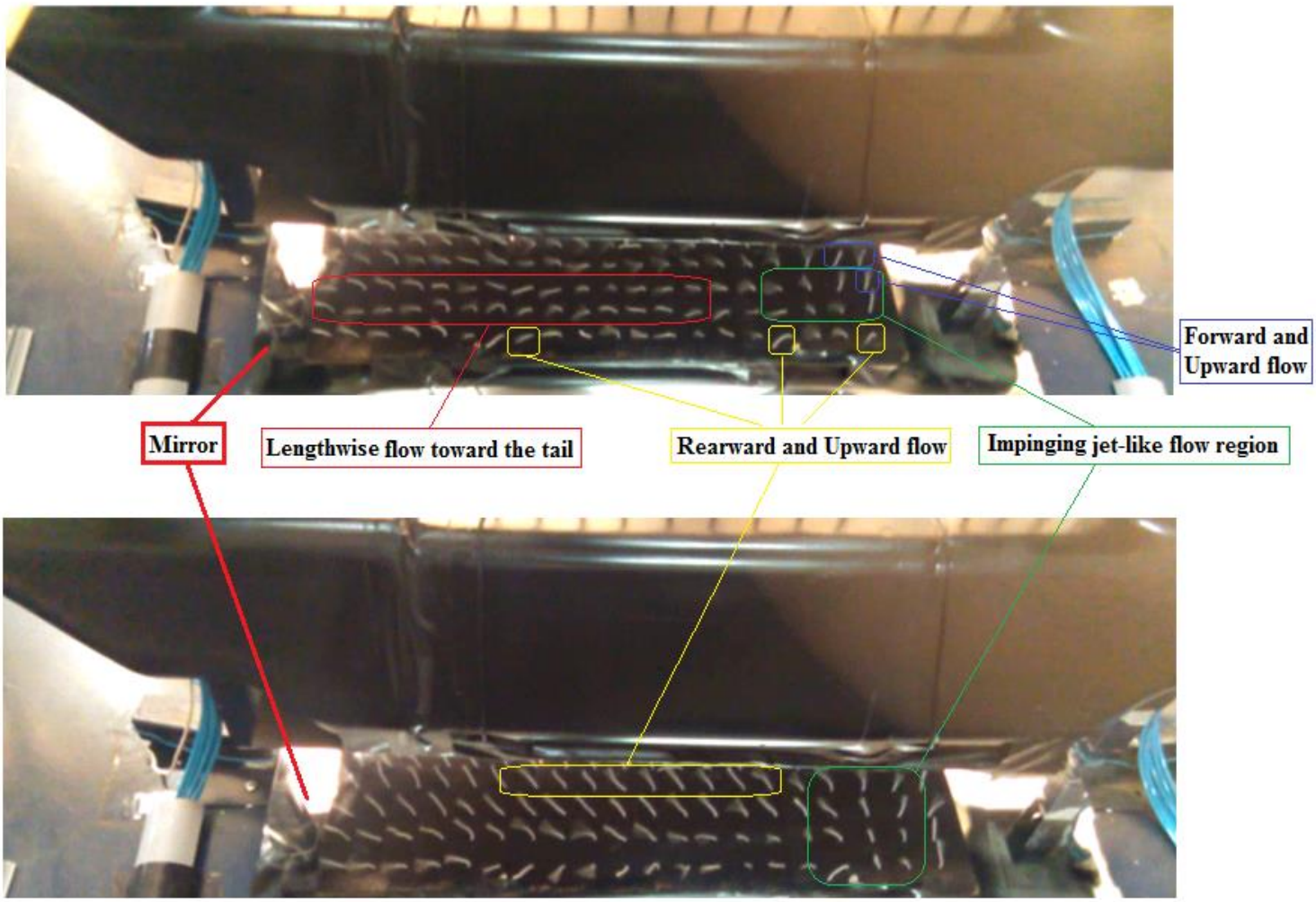

Fig. 12: . Tuft flow visualization of bottom surface for single rotor operation in rpm=2000.

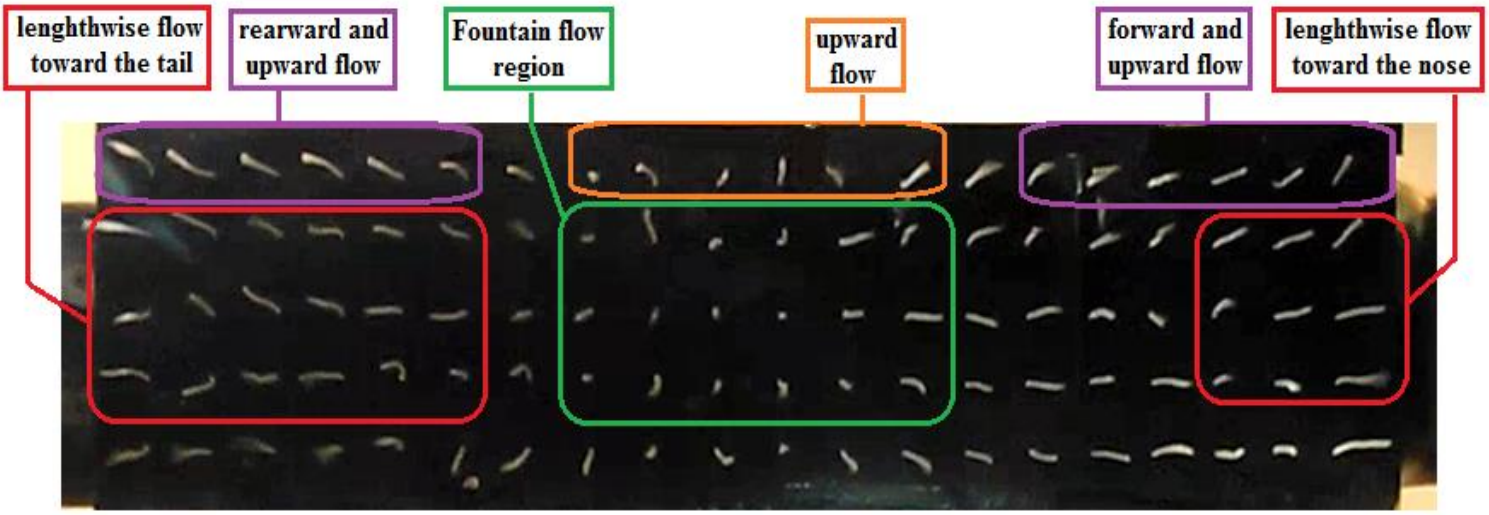

Fig. 13: . Tuft flow visualization of bottom surface for tandem rotor operation in rpm=2000.

the helicopter body was lengthwise flow toward the tail. Since the front rotor was working in this experiment, the outwash flow started at the bottom surface behind the center of this rotor and moved toward the helicopter tail.At some points on the edges of the bottom surface there were rearward and upward flows. These flows were on sidewalls of the airframe due to the pressure difference below and above the body. However, due to the shape of the body and the adverse pressure gradient in the upstream parts of the sidewalls, upward flow may be separated from the sidewall surfaces. Flow separation on the walls creates an almost vacuum area in the upstream areas, so created a positive effect on the overall lift. In the front underneath the body, there was an impinging jet-like small region. As shown in Fig. 8(a), in this area located between x/l=0.2 to 0.4, the pressure value was maximum. It is understood that there was an area that rotor-induced flow was subdivided into forward outwash, backward outwash and upward side flows there.

3.3.2. Tandem Rotor

To study the effect of aerodynamic interaction of tandem rotors on pressure distribution under the body and the formation of fountain flow, the tuft flow visualizations for these configurations were conducted in elevation $h/2R$=0.5 and $h/2R$=1 (Figs.13 and 14).

Fountain flow tuft flow visualization tests conducted for tandem rotors showed that there are some fundamental differences in the behavior of this configuration comparing to the single rotor baseline, as a result of the flow-field due to the rear rotor and the combinational effects of the twin rotors on the induced flow-field. In Fig. 13, it is seen that the semi-quiescent Fountain flow region was located in the central region at bottom of the body(x/l=0.45 to 0.55). It was seen in Fig. 10 that maximum pressure occurred at this region when $h/2R$=1. So, tuft flow visualization experiments confirmed the accuracy of the measurements.

At an elevation of $h/2R$=0.5, the impact flow to the bottom of the body was extremely disturbed due to the longer life of the rotor wake vortices in the wall jet and their oscillatory nature. As a result, the movements and orientations of the tufts were very unstable and fluctuating, so the flow ranges, especially the impacting Fountain flow range, were constantly changed, and detecting the flow pattern was also very difficult. Like as single rotor operation, in this case, there were forward, rearward and upward flows. The cause of such flows was due to the effects of the fountain flow and have positive effects on the lifting force and the aerodynamic performance of the rotors. In Fig. 14, it was seen that there were longitudinal and lateral inward airflow regions below the nose and tail and between the rotors respectively. Tuft flow visualization experiments showed these phenomena at both altitudes for such configurations. The cause of such flows was the effects of the upward fountain flow between the twin-rotor which creates a suction on the central flow.

3.4. Uncertainty Of Results

To measure the uncertainty in this study, tests were repeated five times. The uncertainty of the results is the product of the standard deviation on a value called t-distribution, which is expressed in the form of a table, depending on the number of observations and confidence intervals considered. By calculating the mean and standard deviation of the pressure values

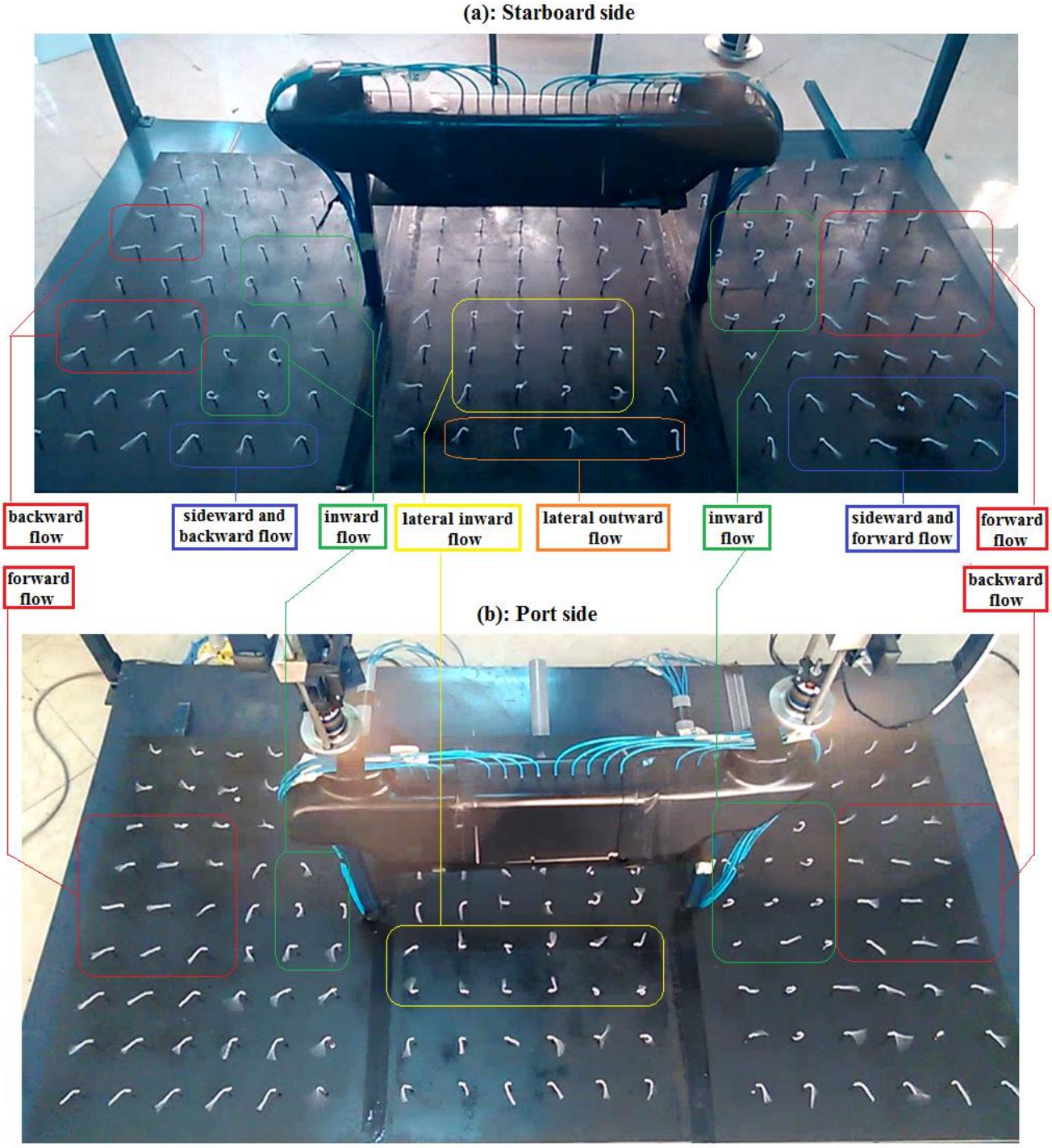

Fig. 14. Tuft flow visualization on the ground for tandem rotors.

measured by ports and the thrust values, and taking into account the 95% confidence interval, the mean uncertainty at the present results was calculated 5.6%. In other words, if the experiments were repeated under the same conditions, probably 95% of new results would be on average 5.6% different from the results presented in this paper. Factors such as interferences caused by sensors working together, error in data transfer terminals, frictional loss due to pneumatic tubes' length, and oscillations caused by rotors are evaluated as factors in the uncertainty of the results. The uncertainty in the measurement is shown in all presented diagrams.

4. CONCLUSIONS

A series of tests have been performed using a multipurpose test stand to study the Fountain flow pattern for both single and tandem rotor configurations at two elevations from the ground surface. The pressure and velocity measurements were performed by the pressure ports drilled longitudinally along the fuselage. The rotors and the fuselage have been scaled from a generic tandem rotor helicopter.

For a single rotor, the results have shown that when the elevation of the rotor increased from $h/2R$=0.5 to $h/2R$=1, the pressure distribution at the bottom surface of the body caused by impact flow decreased and changes in rotational speed of the rotor had almost any significant influence on pressure values. It was also observed that the maximum values of the pressure were recorded in regions below the blade tip and near the middle of the body. Tuft flow visualization showed that when the single rotor was operating, a large part of the flow at bottom of the body, which was affected by outwash flow, was lengthwise toward the tail of the helicopter. In this case, an impinging jet-like small region and rearward and upward flows were underneath the body.

By the addition of the second rotor rotation, the pressure distribution due to the Fountain flow was greatly increased, especially this increase was more significant when the height of rotors and airframe decreased. The location of the maximum pressure under the airframe has changed by varying the model heights.

For tandem rotors configuration there was an area below the airframe where the average velocity was very low there and it can be said that the semi-quiescent flow was there. Tuft flow visualization tests conducted for non-overlapping tandem rotors showed that there were some fundamental differences in flow patterns below these configurations which were caused by Fountain flow formation comparing to the single rotor baseline. Tuft test observations confirmed the location of the Fountain flow formation guessed by results of pressure and velocity measurements and showed that such a flow area existed.

In general, it can be said that the presence of a second rotor in tandem rotor configuration, causes a Fountain flow in the longitudinal center region below the helicopter body and the overlap between the rotors causes a significant increase in pressure values relative to the non-overlapping rotors. This flow has positive effects such as increasing the pressure distribution balance and reinforcing the lift by sub-body pressure and formation of the positive pressure gradient on sidewalls of the airframe.

Nomenclature

h	Rotor elevation from the ground, m
kPa	Kilo Pascal(pressure unit)
l	Body length of the model helicopter, m
ms	Millisecond
mv	Millivolt
p	Pressure, N/m^2
R	The blade radius, m
RMS	Root Mean Square
rpm	Revolution per minute(rotational speed)
v	Impact flow velocity, m/s
x	Longitudinal position, m
z	The vertical distance from the ground, m

Subscript

$_{ref}$	Ambient
$_{rms}$	Root mean square
$_{tip}$	rotor tip

REFERENCES

[1] M. Silva, R. Riser, CH-47D tandem rotor outwash survey, in: AHS 67th Annual Forum, 2011.

[2] USA. Transportation, Department of. 2010, Rotorcraft Flying Handbook.

[3] G.J. Leishman, Principles of helicopter aerodynamics with CD extra, Cambridge university press, 2006.

[4] J.R. Preston, S. Troutman, E. Keen, M. Silva, N. Whitman, M. Calvert, M. Cardamone, M. Moulton, S.W. Ferguson, Rotorwash Operational Footprint Modeling, Missile Research Development and Engineering Center Redstone Arsenal al …, 2014.

[5] F.F. Felker, A review of tilt rotor download research, (1988).

[6] F.F. Felker, J.S. Light, Aerodynamic interactions between a rotor and wing in hover, Journal of the American Helicopter Society, 33(2) (1988) 53-61.

[7] M. MCVEIGH, The V-22 tilt-rotor large-scale rotor performance/wing download test and comparison with theory, Vertica, 10(3) (1986) 281-297.

[8] D.R. Polak, W. Rehm, A.R. George, Effects of an image plane on the tiltrotor fountain flow, Journal of the American Helicopter Society, 45(2) (2000) 90-96.

[9] M. Ramasamy, M. Potsdam, G.K. Yamauchi, Measurements to Understand the Flow Mechanisms Contributing to Tandem-Rotor Outwash, (2018).

[10] V. Gupta, J.D. Baeder, Quad tilt rotor aerodynamics in helicopter mode, in: Annual Forum Proceedings-American Helicopter Society, American Helicopter Society, INC, 2005, pp. 416.

[11] M. Ramasamy, J.G. Leishman, Interdependence of diffusion and straining of helicopter blade tip vortices, Journal of Aircraft, 41(5) (2004) 1014-1024.

[12] B. Johnson, J.G. Leishman, A. Sydney, Investigation of Sediment Entrainment Using Dual-Phase, High-Speed Particle Image Velocimetry, Journal of the American Helicopter Society, 55(4) (2010) 42003-42003.

[13] 24-ft Wind Tunnel Tests of Model Multi-Rotor Helicopters, RAE Report No. Aero 2207, 1947.

[14] A. Halliday, D. Cox, Wind Tunnel Experiments on a Model of a Tandem Rotor Helicopter, HM Stationery Office, 1961.

[15] J.-f. Tan, H.-w. Wang, Simulating unsteady aerodynamics of helicopter rotor with panel/viscous vortex particle method, Aerospace Science and Technology, 30(1) (2013) 255-268.

[16] Y. You, D. Na, S.N. Jung, Improved rotor aeromechanics predictions using a fluid structure interaction approach, Aerospace Science and Technology, 73 (2018) 118-128.

[17] A. Antoniadis, D. Drikakis, B. Zhong, G. Barakos, R. Steijl, M. Biava, L. Vigevano, A. Brocklehurst, O. Boelens, M. Dietz, Assessment of CFD methods against experimental flow measurements for helicopter flows, Aerospace Science and Technology, 19(1) (2012) 86-100.

[18] G.M. Eberhart, Modeling of Ground Effect Benefits for Multi-Rotor Small Unmanned Aerial Systems at Hover, Ohio University, 2017.

[19] [19] H. Tadghighi, R.G. Rajagopalan, A user's manual for ROTTILT solver: Tiltrotor fountain flow field prediction, (1999).

[20] L. Ye, Y. Zhang, S. Yang, X. Zhu, J. Dong, Numerical simulation of aerodynamic interaction for a tilt rotor aircraft in helicopter mode, Chinese Journal of aeronautics, 29(4) (2016) 843-854.

[21] J.F. Tan, T.Y. Zhou, Y.M. Sun, G.N. Barakos, Numerical investigation of the aerodynamic interaction between a tiltrotor and a tandem rotor during shipboard operations, Aerospace Science and Technology, 87 (2019) 62-72.

[22] F. Shahmiri, Experimental Investigation of the Hovering Performance of a Twin-Rotor Test Model, Journal of Aerospace Science and Technology (JAST), 10(2)(2013) 1-7.

[23] A.M. Radhakrishnan, An experimental investigation of ground effect on a quad tilt rotor in hover and low speed forward flight, 2006.

[24] Q. Wang, Q. Zhao, Rotor aerodynamic shape design for improving performance of an unmanned helicopter, Aerospace Science and Technology, 87 (2019) 478-487.

[25] A.J. Wadcock, L.A. Ewing, E. Solis, M. Potsdam, G. Rajagopalan, Rotorcraft downwash flow field study to understand the aerodynamics of helicopter brownout, National Aeronautics and Space Administration Moffett Field Ca Ames Research …, 2008.

[26] H. Tennekes, J.L. Lumley, J.L. Lumley, A first course in turbulence, MIT press, 1972.

HOW TO CITE THIS ARTICLE

A. Mehrabi, A. R. Davari, Assessment of Fountain Flow Effects on Two Non-Overlap Tandem Rotors Performance, AUT J. Mech. Eng., 5(1) (2021) 173-190.

DOI: 10.22060/ajme.2020.17224.5850